Excited-State Photoreactions of Chlorine Dioxide in Water

Robert C. Dunn and John D. Simon*

Contribution from the Department of Chemistry, University of California at San Diego, 9500 Gilman Drive, La Jolla, California 92093-0341. *Received December 2, 1991*

Abstract: The primary photochemical processes of electronically excited OClO in water are studied at room temperature. Excitation of the $^2A_2 \leftarrow {}^2B_1$ absorption band at 355 nm leads to both photochemical dissociation and isomerization, yielding ClO + O and ClOO, respectively. The isomerized ClOO is unstable in water and thermally dissociates into Cl and O_2. A kinetic model is developed to quantify the partitioning between these two competitive processes. Comparison between experimental and simulated transient absorption data shows that 90% of the electronically excited molecules dissociate; the remaining 10% undergo isomerization to form ClOO. In addition, the simulated kinetics show that the thermal decomposition of ClOO in water has a rate constant of 6.7×10^9 s^{-1}.

Introduction

The past decade has seen a considerable growth in research concerned with the photochemistry of chlorine oxides due to their increasingly prevalent role in the Antarctic ozone problem.[1] As a result of these efforts, a large database now exists for the chemical reactivity of many small chlorine oxides.[2] In a few cases, both theory and experiment have advanced the current understanding to a point where it is now possible to quantitatively describe the potential energy surfaces driving the photochemistry. One such molecule is chlorine dioxide (OClO). While a great deal of experimental research on OClO in both the gas phase[3-9] and matrix[10-12] has been reported, surprisingly little has been done on OClO in solution.[13,14] The reactive nature of the intermediates formed, along with their relatively small absorptivities, has no doubt played a role. In this paper, we report a complete study of the primary photoprocesses that occur when OClO is electronically excited in water solution.

Chlorine dioxide exists in two isomeric forms: the symmetric OClO and the asymmetric ClOO. The ClOO isomer is thermodynamically more stable than OClO by ~3 kcal/mol.[15] However, the ClOO isomer is very reactive and has been difficult to study spectroscopically. Fortunately, OClO is kinetically stable at room temperature, showing no thermal reactivity in water over periods of days.[14] Comprehensive experimental and theoretical studies of OClO reveal a complex photoreactivity involving several excited-state potential energy surfaces.[6-8,15-17] Gas-phase experiments show that excitation in the near-UV region results in either bond breakage to form vibrationally excited ClO and atomic oxygen or isomerization to form the reactive ClOO molecule.[6-9,17] The isomerized product fragments into oxygen and atomic chlorine.[6,17] This overall excited-state photochemistry is represented by the two competitive pathways shown in eq 1.

$$\mathrm{OClO} + h\nu \rightarrow \mathrm{OCl} + \mathrm{O} \qquad (1)$$
$$\rightarrow \mathrm{ClOO} \rightarrow \mathrm{Cl} + \mathrm{O_2}$$

This complex photochemistry is thought to be controlled by three closely spaced excited-state electronic surfaces.[15] Excitation populates the bound $^2A_2$ state. In the gas phase, the direct absorption spectrum ($^2A_2 \leftarrow {}^2B_1$) is highly structured and spans the near-UV region from 260 to 480 nm.[6,7,18] Nearby in energy to the excited $^2A_2$ state are two additional excited states ($^2B_2$ and $^2A_1$). Transitions to the $^2B_2$ state are dipole forbidden.[15] Absorption to the $^2A_1$ state is symmetry allowed. However, it is a perpendicular transition and weaker than the parallel transition to the $^2A_1$ state. No experimental observations of the $^2A_1 \leftarrow {}^2B_1$ absorption have been reported. These states are not observed spectroscopically but participate in the excited-state chemistry of this molecule. These states give rise to the two photoreactions shown in eq 1. Coupling to the low-lying $^2B_2$ excited state gives rise to dissociation into O and vibrationally hot ClO. The $^2A_1$ state is dissociative, forming O_2 and Cl, presumably via the photoisomerized intermediate ClOO.[6,9,15] In the gas phase, the partitioning between these two pathways is dependent on excitation wavelength.[8]

Gas-phase quantum yields for the two photoreactive channels are still under debate due to the extreme reactivity of the ClOO isomer. The reported gas-phase quantum yield for isomerization is ~15% for photolysis at 362 nm.[17] In contrast, the photochemistry of OClO in matrices of argon,[10,11] nitrogen,[11] and sulfuric acid[12] is reported to lead exclusively to the ClOO isomer when excited near the maximum of the near-UV transition. In a matrix, cage effects can influence product formation. The rigidity of the matrix may prevent the formation of stable bimolecular products such as ClO and O. This would give the appearance of forming only the thermodynamically more stable ClOO isomer. The extent of this isomerization channel is important since it leads to the formation of Cl, which has been linked to the catalytic destruction of stratospheric ozone.[1]

In solution, the degree to which OClO decays through isomerization and what effects solvent may have on this reactivity have not been studied. Unlike matrices, the solvent cage is dynamic, and a branching ratio between the two pathways is expected. This branching will depend on both static and dynamic properties of the liquid. The relative efficiency of the reaction channels will

(1) Molina, M. J.; Rowland, F. S. *Nature (London)* **1974**, *249*, 819. Solomon, S.; Mount, G. H.; Sanders, R. W.; Schmeltekopf, A. L. *J. Geophys. Res.* **1987**, *92*, 8329. Solomon, S. *Rev. Geophys.* **1988**, *26*, 131. Anderson, J. G.; Brune, W. R.; Chan, R. J. *J. Geophys. Res.* **1989**, *94*, 11480.
(2) Watson, R. T. *J. Phys. Chem. Ref. Data* **1977**, *6*, 871.
(3) Michielsen, S.; Merer, A. J.; Rice, S. A.; Novak, F. A.; Freed, K. F.; Hamada, Y. *J. Chem. Phys.* **1981**, *74*, 3089.
(4) Hamada, Y.; Merer, A. J.; Michielsen, S.; Rice, S. A. *J. Mol. Spectrosc.* **1981**, *86*, 499.
(5) Glowina, J. H.; Misewich, J.; Sorokin, P. P. In *Supercontinuum Lasers*; Alfano, R. R., Ed.; Springer: Berlin, 1989.
(6) Ruhl, E.; Jefferson, A.; Vaida, V. *J. Phys. Chem.* **1990**, *94*, 2990.
(7) Richard, E. C.; Vaida, V. *J. Chem. Phys.* **1991**, *94*, 153.
(8) Richard, E. C.; Vaida, V. *J. Chem. Phys.* **1991**, *94*, 163.
(9) Vaida, V.; Solomon, S.; Richard, E. C.; Ruhl, E.; Jefferson, A. *Nature* **1989**, *342*, 405.
(10) Rochkind, M. M.; Pimentel, G. C. *J. Chem. Phys.* **1967**, *46*, 4481.
(11) Arkell, A.; Schwager, F. *J. Am. Chem. Soc.* **1967**, *89*, 5999.
(12) Adrian, F. J.; Bohandy, J.; Kim, B. F. *J. Chem. Phys.* **1986**, *85*, 2692.
(13) Dunn, R. C.; Richard, E. C.; Vaida, V.; Simon, J. D. *J. Phys. Chem.* **1991**, *95*, 6060.
(14) Dunn, R. C.; Flanders, B. N.; Vaida, V.; Simon, J. D. *Spectrochim. Acta*, in press.
(15) Gole, J. L. *J. Phys. Chem.* **1980**, *84*, 1333.
(16) (a) Colussi, A. C. *J. Phys. Chem.* **1990**, *94*, 8922. (b) Colussi, A. J.; Redmond, R. W.; Scaiano, J. C. *J. Phys. Chem.* **1989**, *93*, 4783.
(17) Bishenden, E.; Hancock, J.; Donaldson, D. J. *J. Phys. Chem.* **1991**, *95*, 2113.
(18) Wahner, A.; Tyndall, G. S.; Ravishankara, A. R. *J. Phys. Chem.* **1987**, *91*, 2734.

0002-7863/92/1514-4856$03.00/0

be dependent upon both the positions of the curve crossings between the excited states and the magnitudes of their coupling.[7-9] Since the charge distributions of the reactive $^2B_2$ and $^2A_1$ states are different from each other and from the Franck–Condon populated $^2A_2$ state,[15] the chemistry will be very sensitive to dielectric properties of the liquid. In this paper, the photochemistry of OClO in water is examined. Through the time evolution of the absorption properties of the system, a quantitative model of the dual channel photochemistry is developed.

Experimental Section

The time-dependent absorption signals were recorded using a kilohertz repetition rate picosecond laser system, the details of which can be found elsewhere.[19] Briefly, a mode-locked, Q-switched and cavity-dumped continuous wave Nd:YAG laser was used to synchronously pump a tunable cavity-dumped dye laser. The cavity-dumped infrared pulses from the YAG oscillator were tripled to 355 nm (20 μJ/pulse) and used as the photolysis pulses in a simple pump–probe experimental arrangement. Probe pulses at 266 nm and from 280 to 440 nm were generated by doubling the leftover 532-nm pulses from the cavity-dumped YAG and by doubling the output of the cavity-dumped dye laser, respectively. To generate the probe pulses in the 230–260-nm region, a combination of LBO crystals was used to produce sufficient third harmonic (355 nm) to pump a cavity-dumped blue dye laser. The output of the dye laser was doubled in β-BBO to cover the desired spectral range. All laser beams were depolarized to remove any coherence- or polarization-dependent artifacts that might interfere with the signals. The probe beam was detected by a PMT, amplified, and sent to a boxcar integrator (SRS Model 250). The output of the boxcar integrator was sent to a lock-in amplifier (EG&G Model 5209), which was referenced to a 500-Hz chopper placed in the photolysis beam. The output from the lock-in was processed by an IBM-PC/AT computer. A computer-controlled digital delay line (Velmex) was used to scan the delay time between pump and probe pulses. Cross correlation measurements gave an instrument response function of 80 ps.

Chlorine dioxide was initially generated by flowing chlorine gas through a column of sodium chlorite ($NaClO_2$).[20] This procedure generated OClO by the following reaction.

$$2ClO_2^- + Cl_2 \rightarrow 2Cl^- + 2OClO \quad (2)$$

The gaseous OClO product was subsequently bubbled through a water sample. This method, however, resulted in solutions that contained a significant amount of unreacted Cl_2. Chlorine absorbs in the same region as OClO.[21] The photoinduced dynamics associated with the dissociation and recombination of Cl_2 produced large absorption signals that rendered the study of OClO impossible.

To remedy this, the synthetic method reported by Bray[22] for producing chlorine dioxide from oxalic acid and potassium chlorate was used. Oxalic acid (30 g) was thoroughly mixed with 8 g of potassium chlorate and placed in a 500-mL, two-necked, round-bottomed flask. Approximately 4 mL of water was added to the flask. The solution was placed in a water bath and heated to 50–60 °C to initiate the reaction shown below.

$$2ClO_3^- + H_2C_2O_4 \rightarrow 2OH^- + 2CO_2 + 2OClO \quad (3)$$

Nitrogen was passed over the reaction mixture, and the gases were bubbled through a 4-L container of water to dissolve the OClO and CO_2 that evolved over an approximately 2-h period. As carbon dioxide does not absorb in the spectral region studied, this method provides optically pure OClO samples. The resulting concentration of aqueous OClO was ~2 M.[23]

Samples were flowed through a quartz sample cell with a 2-mm path length. Early experiments used a closed cycle circulating system, which unfortunately led to artifacts in the signal due to the buildup of photoproducts, mostly Cl_2. To avoid this, 4-L solutions were prepared for each probe wavelength studied. The sample was flowed through the cell at a rate which guaranteed that each laser shot was exposed to fresh solution. As a result, data acquisition was limited to the time it took for the 4-L sample to flow through the cell, ~6 min. To obtain the signal-to-noise levels necessary for a quantitative analysis of the data, this limited the longest possible delay between the pump and probe beams to 2.5–3 ns. Longer delays were possible with larger volume solutions.

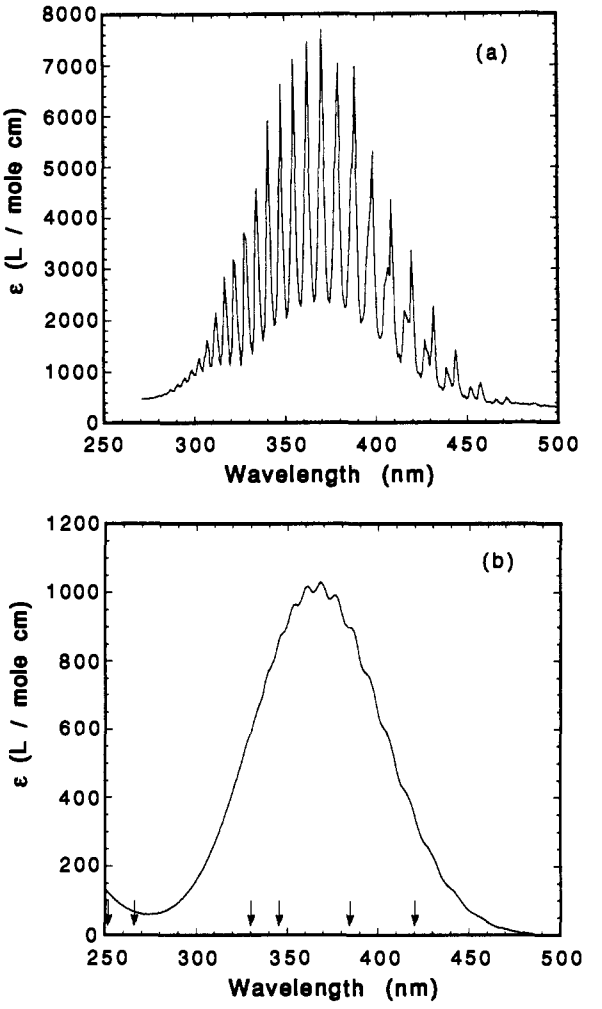

Figure 1. Electronic absorption spectra of the $^2A_2 \leftarrow {}^2B_1$ transition of (a) gaseous and (b) aqueous OClO at room temperature. Extinction coefficients are taken from refs 18 and 24, respectively.

Results and Discussion

Spectra of Reactive Intermediates. In the absence of reaction with solvent, the photochemistry of OClO produces the following chemical species: ClO, O, Cl, O_2, and ClOO. In order to interpret time-dependent absorptions, the spectral properties of these molecules are required. In the experiments reported, dynamics were examined for probe wavelengths between 230 and 440 nm. Two of the potential photoproducts, O and O_2, do not absorb in this range. Before examining time-dependent data, the spectra of the remaining intermediates are characterized.

Figure 1 shows the gas-phase and solution near-UV $A^2A_2 \leftarrow X^2B_1$ absorption spectra of OClO. Both spectra reveal similar absorption maxima and vibronic structure of comparable spacings,[14] which indicates that solvation has only a small solvent effect on the excited-state potential. The maximum absorption of the solvated molecule occurs at 370 nm. The extinction coefficient at this wavelength is ~1050 L/(mol cm),[24] decreased by ~85% from that reported for the gas phase.[18] The $A^2A_2 \leftarrow X^2B_1$ absorption spectrum of OClO also shifts in different solvents.[14] This is not surprising as OClO is a dipolar molecule and electrostatic interactions should influence the absorption band. In polar solvents, the absorption shifts are small, spanning 200 cm^{-1} in changing the solvent from 2-pentanol (ϵ = 13.8; $E_T(30)$ = 46.5 kcal/mol) to water (ϵ = 78.4; $E_T(30)$ = 63.1 kcal/mol).[14] A complete discussion of solvent effects on the absorption spectrum

(19) Xie, X.; Simon, J. D. *Opt. Commun.* **1989**, *69*, 303.
(20) Derby, R. I.; Hutchinson, W. S. *Inorg. Synth.* **1953**, *4*, 152.
(21) Simon, F. G.; Burrows, J. P.; Schneider, W.; Moortgat, G. K.; Crutzen, P. J. *J. Phys. Chem.* **1989**, *93*, 7807.
(22) Bray, W. *Z. Phys. Chem.* **1906**, *54*, 569. Babcock, L. M.; Pentecost, T.; Koppenol, W. H. *J. Phys. Chem.* **1982**, *93*, 8126.
(23) *CRC Handbook of Chemistry and Physics*; CRC Press: Cleveland, OH, 1990.
(24) Stitt, F.; Friedlander, S.; Lewis, H. J.; Young, F. E. *Anal. Chem.* **1954**, *26*, 1478.

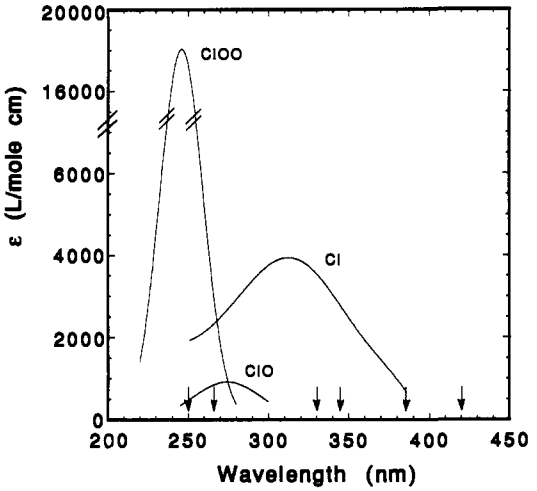

Figure 2. Electronic absorption spectra of aqueous ClO, Cl, and gas-phase ClOO adapted from reported literature values.[25-27]

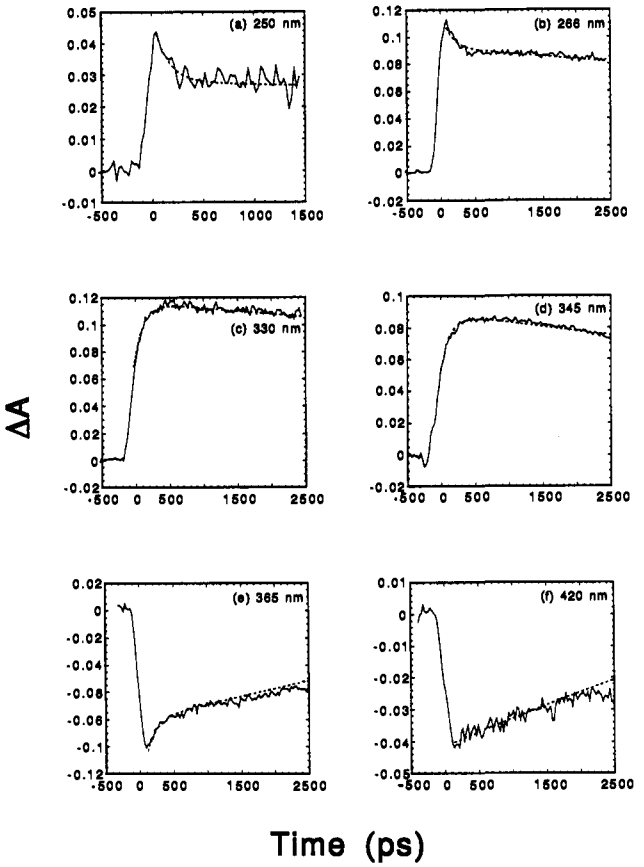

Figure 3. Time-resolved absorption dynamics following the excitation of OClO in water at 355 nm. The dynamics were recorded at 16 probe wavelengths between 230 and 440 nm. The data shown in a–f are representative of the range of dynamics observed. Dashed lines represent a fit based on the kinetic model described in the text.

of OClO has recently appeared.[14]

A solution spectrum of ClOO has not been reported. In part, this is due to the reactivity of this molecule, rendering it difficult to isolate for study. However, extensive gas-phase measurements have been carried out, and the absolute cross section and spectral shape are known.[25,26] Aqueous Cl and ClO have been characterized spectroscopically.[27] In Figure 2, the absorption spectra of solvated ClO and Cl and gas-phase ClOO are shown. These data are redrawn from the cited literature references. The spectra of these three potential intermediates overlap in some regions of the spectrum but are well separated in others. The strongest absorber is ClOO, with an absorption approximately twice as intense as the gaseous OClO spectrum.

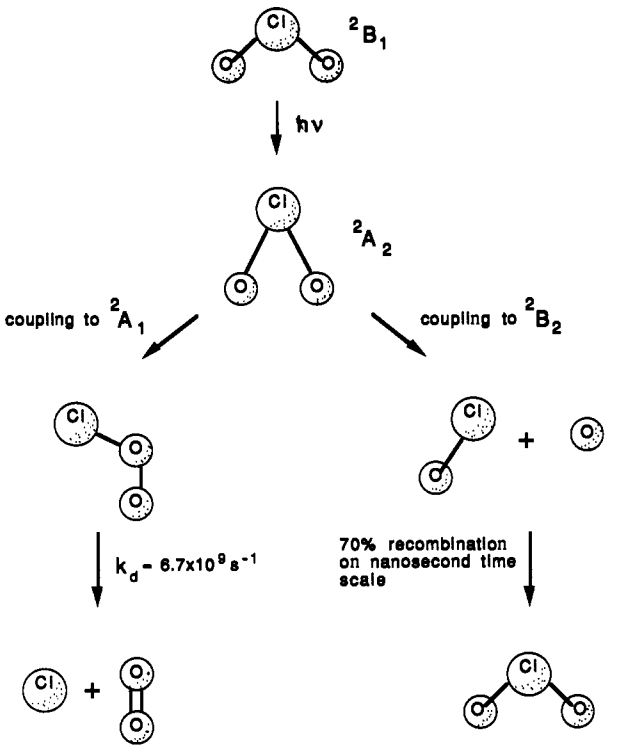

Figure 4. Schematic diagram showing the steps involved in the photodissociation of aqueous OClO. Upon excitation at 355 nm, 90% of the excited OClO undergoes photodissociation forming ClO + O, of which 70% re-forms OClO on the nanosecond time scale. The remaining 10% of the excited OClO isomerizes to ClOO. This species is kinetically unstable at room temperature and thermally decomposes into Cl + O_2 with a rate constant $k_d \sim 6.7 \times 10^9\ s^{-1}$. The proposed couplings between the electronically excited $^2A_2$ state and the nearby $^2A_1$ and $^2B_2$ electronic states are based on reported gas-phase studies.[6,9]

Transient Absorption Dynamics. Figure 3 shows time-resolved absorption dynamics following the excitation of OClO at 355 nm for several wavelengths in the region from 230 to 440 nm. These data demonstrate the range of kinetic behaviors observed. Probing at 250 nm (Figure 3a), an initial instrument-limited increase in absorption follows photolysis. This is followed by a decay in the signal within the first 200 ps, after which a constant transient level is observed. The time-dependent signal at 266 nm (Figure 3b) shows similar behavior. However, at this wavelength, the relative magnitude of the long-time signal to that observed immediately after excitation is greater than that found at 250 nm. At 330 nm (Figure 3c), the signal also rises within the instrument response. However, this is now followed by a time-dependent increase in signal. The transient absorption reaches a maximum at ≈500 ps, after which it slowly decays to ≈95% of its maximum value by 2.5 ns. Similar behavior is also seen when probing at 345 nm (Figure 3d). At this wavelength, the nanosecond decay component is more pronounced, with the signal decreasing to ≈85% of the maximum value by 2.5 ns. Tuning the probe wavelength to 385 nm produces the transient kinetics shown in Figure 3e. At this wavelength, an absorption bleach is observed upon photoexcitation. The signal recovery exhibits two components, one occurring during the first few hundred picoseconds, the other requiring nanoseconds. Probing at a lower energy, e.g., 420 nm, also results in an initial

(25) Morris, E. D.; Johnston, H. S. *J. Am. Chem. Soc.* **1968**, *90*, 1918. Johnston, H. S.; Morris, E. D.; Van den Bogaerde, J. *J. Am. Chem. Soc.* **1969**, *91*, 7712.

(26) Mauldin, R. L., III; Burkholder, J. B.; Ravishankara, A. R. *J. Phys. Chem.* **1992**, *96*, 2582.

(27) Klaning, U. K.; Wolff, T. *Ber. Bunsen-Ges. Phys. Chem.* **1985**, *89*, 243.

bleach (Figure 3f). However, unlike the 385-nm data, the signal recovery involves only a nanosecond component.

The wavelengths plotted in Figure 3 are indicated by the arrows in Figures 1 and 2. These show that the data probe different combinations of the possible reactive intermediates that are formed by photolysis of OClO. In total, 16 wavelengths were probed between 230 and 440 nm. Several qualitative statements can be made about the data set. First of all, in the region where only OClO absorbs, $\lambda > 400$ nm, a signal bleach is observed which has a single recovery component. This is exemplified by Figure 3f; the dynamics in this region are also wavelength independent. Similar nanosecond components are observed throughout the near-UV region where ClO absorbs. However, in this region, the data show a time-dependent absorption decrease. Second, through the entire region where ClOO and Cl absorb, a picosecond component is observed, leading to absorption increases in the region from 300 to 400 nm and decreases from 240 to 290 nm. Thus, the data clearly contain two kinetic processes. The first occurs within the first few hundred picoseconds. The second takes place over several nanoseconds.

Kinetic Model. In modeling the photoreactions of OClO in solution, two competing processes need to be included. First, the molecule can dissociate into ClO and O.[5,6,16] Following dissociation, recombination to form OClO (or ClOO) will compete with generation of free ClO and O.[28] The second process involves initial isomerization to form ClOO, followed by thermal decomposition into Cl and O_2.[6,17] As shown in Figures 1 and 2, the spectra of these reaction products are known. Thus, time-dependent absorption kinetics can be calculated once a model for the kinetics is assumed. For nanosecond kinetics, it is not necessary to consider the thermal reactions of Cl, ClO, and OClO with water.[14,27]

The simplest kinetic model for describing the photochemistry of OClO in solution is shown in Figure 3. From the gas-phase spectroscopy, insight into the time scales associated with the primary bond breakage and isomerization event can be obtained. Line-width measurements suggest that the excited-state lifetime is on the order of 1 ps.[7,8] Within the time resolution of the current experiment, the partitioning between predissociation to form ClO and O and isomerization to form ClOO will occur within the instrument response. Thus, at time $t = 0$, it is reasonable to assume an initial concentration of ClO and ClOO, which together equal the concentration of OClO which is photolyzed. The kinetics associated with the formation of these initial concentrations is not manifested in the transient absorption data. Once formed, the following reactions need to be included.

$$\mathrm{ClOO} \xrightarrow{k_d} \mathrm{Cl} + \mathrm{O_2} \tag{4}$$

$$\mathrm{ClO} + \mathrm{O} \xrightarrow{k_{rec}} \mathrm{OClO} \tag{5}$$

Equation 5 competes with the formation of free ClO and O and, for the time scales probed, represents the recombination yield. It is also possible that ClO and O will recombine to form the reactive ClOO isomer. However, no increases in chlorine signals ($\lambda \sim 330$ nm, Figure 3c) are observed on the same time scales as the recovery of the OClO absorption ($\lambda \sim 420$ nm, Figure 3f). Thus, this process is not included in the kinetic model. In this simple model, the time-dependent concentrations of the reactive intermediates that absorb in the region between 230 and 440 nm can be obtained. These are given by eqs 6–9,

$$[\mathrm{ClOO}](t) = [\mathrm{ClOO}]_0 \exp(-k_d t) \tag{6}$$

$$[\mathrm{Cl}](t) = [\mathrm{ClOO}]_0 \{1 - \exp(-k_d t)\} \tag{7}$$

$$[\mathrm{ClO}](t) = [\mathrm{ClO}]_{rec}(t) + [\mathrm{ClO}]_{sep} \tag{8}$$

$$[\mathrm{OClO}](t) = [\mathrm{ClO}]_{rec(0)} - [\mathrm{ClO}]_{rec}(t) \tag{9}$$

where

$$[\mathrm{ClO}]_{rec}(t) = \frac{[\mathrm{ClO}]_{rec(0)}}{1 + 2k_{rec}t[\mathrm{ClO}]_{rec(0)}} \tag{10}$$

(28) Harris, A.; Berg, M.; Harris, C. *J. Chem. Phys.* **1986**, *84*, 788.

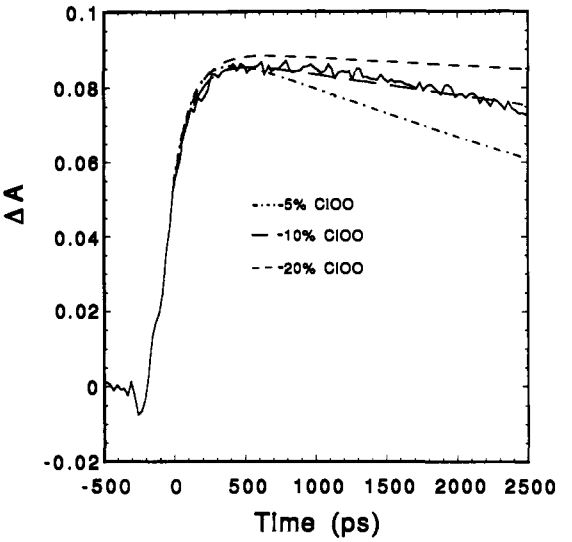

Figure 5. Effects on the simulated data at 345 nm when the partitioning between the dissociation and isomerization channels is varied. The optimal fit to the entire data set is obtained when 10% of the excited molecules undergo isomerization. As exemplified here, small changes in this ratio result in observable deviations from the measured dynamics.

In these equations, the initial concentration of ClO, $[\mathrm{ClO}]_0$, that is formed by dissociation is partitioned into two fractions, those that undergo recombination, $[\mathrm{ClO}]_{rec}(t)$, and those that escape, $[\mathrm{ClO}]_{sep}$. This gives rise to the constraint given by eq 11.

$$[\mathrm{ClO}]_0 = [\mathrm{ClO}]_{rec(0)} + [\mathrm{ClO}]_{sep} \tag{11}$$

There are four parameters in the kinetic model. First, the partitioning between dissociation and isomerization. Second, the reaction rate constant for the thermal decomposition of ClOO, k_d. Third, the partitioning of ClO between recombination and escape, $[\mathrm{ClO}]_{rec}$ and $[\mathrm{ClO}]_{sep}$, respectively. Fourth, the bimolecular reaction rate constant for recombination of ClO and O to form OClO, k_{rec}.

The time-dependent concentrations of these intermediates can be used to calculate transient absorption dynamics. This is done using eq 12, where the summation runs over the i different chemical intermediates (ClOO, ClO, Cl, and OClO).

$$A(\lambda,t) = \sum_i \epsilon(\lambda)[i](t) \tag{12}$$

The four kinetic parameters were varied to provide the best global fit of eq 12 to the 16 transient absorption decays collected through the spectral region from 230 to 440 nm. The dashed lines in Figure 3 represent the best fits obtained. The entire set of absorption data could be quantitatively described by a single set of parameters. Optimization of the fits reveals that, within 10 ps after photoexcitation, 90% of the excited OClO molecules dissociate into ClO and O, of which 70% undergo recombination on the nanosecond time scale. The remaining 10% of the initially excited OClO molecules form ClOO. The subsequent thermal decomposition of ClOO in room temperature water to form free Cl and O_2 has a reaction rate constant of $\sim 6.7 \times 10^9$ s^{-1}.

The sensitivity of the fits to changes in the partitioning between the initial dissociation and isomerization is demonstrated in Figure 5 using the data from 345 nm. Changes on the order of a few percent result in observable deviations between the experimental and calculated curves. Thus, the ability of one set of parameters to quantitatively account for the 16 experimental data sets indicates that the resulting partitioning is accurate to better than ±3%. It is important to recall at this point that the spectrum used for ClOO was that obtained from recent gas-phase measurements.[25,26] In computing the calculated curves, the ClOO spectrum contributes within the first few hundred picoseconds and only at wavelengths below ~280 nm. After a few hundred picoseconds, only the Cl atoms give rise to absorption signals. In principle, the relative yields of isomerization and dissociation can be esti-

mated from the kinetics of formation of Cl, in spectral regions where only Cl and ClO contribute. The ability to reproduce both the short-time dynamics and the long-time signal levels implies that the solution-phase spectrum of ClOO is very similar to that in the gas phase. Changes on the order of ±10% in extinction coefficient for this reactive molecule do not affect the conclusion drawn above.

Although the above model accurately describes the observed dynamics, one additional factor needs to be discussed. From gas-phase studies, it has been shown that the photodissociated ClO molecule is vibrationally hot.[5,6,16] In solution, vibrational cooling is known to result in spectral shifts, which can lead to complicated transient absorption kinetics when probing at a single wavelength.[28]

The dynamics of vibrational cooling of small molecules in solution is currently being studied by many research groups.[28-30] One of the best studied chemical systems is the vibrational cooling of I_2.[28] In these experiments, a short light pulse dissociates the iodine molecule. Subsequent geminate recombination produces a vibrationally hot diatomic, which then undergoes relaxation, resulting in a time-dependent blue shift in the absorption spectrum. In the case of probing at individual wavelengths, the relaxation process is reflected by fast transient components which are wavelength dependent. Average relaxation times for I_2 in liquids are on the order of 100 ps.[28] In addition to these studies, recent infrared pump–infrared probe studies by Hochstrasser and co-workers on vibrational relaxation in the azide ion, N_3^-, show that vibrational relaxation from $v = 1$ to $v = 0$ in water occurs within 3 ps.[29] Vibrational relaxation in large dye molecules is also reported to occur in a few picoseconds; however, unlike ClO, these systems have a large number of vibrational degrees of freedom.[30]

In contrast to I_2 or N_3^-, ClO is a dipolar diatomic. Molecular dynamics simulations indicate that dipolar diatomics should exhibit significantly faster vibrational relaxation than that observed for an apolar molecule.[31] The possible involvement of vibrational relaxation of ClO in the observed transient absorption signals can be ruled out, as the time constants for the picosecond absorption decays observed throughout the near-UV region are identical within experimental error. If vibrational relaxation were occurring, redder wavelengths would relax more rapidly.[28] In addition, the fast components observed for the probe wavelengths 330 and 345 nm are in a region where ClO does not absorb. If these are hot-band absorptions, the signal would be expected to quickly decay to zero as the ClO absorption spectrum shifted to the blue. The picosecond component to the transient data set is inconsistent with a mechanism in which excited OClO produces vibrationally hot ClO which then cools on the 100-ps time scale. It is likely that ClO undergoes relaxation on the subpicosecond to a few picosecond time scale. Studies using femtosecond time resolution are under way to address the vibrational states of this photofragment immediately upon bond breakage.

Conclusions

This paper reports transient absorption experiments on the photochemistry of OClO in room temperature water solution. Following excitation of the $^2A_2 \leftarrow {}^2B_1$ absorption band at 355 nm, the excited OClO molecule undergoes competitive bond dissociation to form ClO + O (90%) and isomerization to form ClOO (10%). The isomerized product thermally dissociates into Cl and O_2 with a first order reaction rate constant of 6.7×10^9 s^{-1}. The percentage of excited molecules that undergo isomerization is consistent with recent gas-phase measurements of 15% Cl atom formation after photoexcitation of ClOO at 362 nm.[17]

Acknowledgment. This work is supported by the National Science Foundation, Division of Experimental Physical Chemistry, and the MMFEL program administered by the Office of Naval Research. We thank Professor Veronica Vaida for many stimulating and informative discussions. We also thank Dr. Floyd Davis and Professor Y. T. Lee for a preprint of their work.

Note Added in Proof. Recently, Davis and Lee[32] reexamined the gas-phase quantum yield for photogeneration of Cl + O_2 using photofragment translational energy spectroscopy. For photolysis at 362 nm, Davis and Lee[32] report a quantum yield of less than 0.2%. This yield is similar to that reported by Lawrence et al.[33] but significantly smaller than that reported by Bishenden and co-workers.[17] The yields of Cl + O_2 reported by Lawrence et al.[33] and Davis and Lee[32] are less than that found for photolysis of OClO in water. Femtosecond experiments are currently in progress to quantify the contributions of excited-state isomerization (via coupling to the $^2A_1$ state) and ultrafast cage recombination of ClO and O to the ClOO signals observed in solution.

Registry No. OClO, 10049-04-4; ClO, 14989-30-1; O, 7791-21-1; ClOO, 17376-09-9; Cl, 22537-15-1; O_2, 7782-44-7.

(29) Owrutsky, J. C.; Kim, Y. R.; Li, M.; Sarisky, M. J.; Hochstrasser, R. M. *Chem. Phys. Lett.* **1991**, *184*, 368.
(30) Laermer, F.; Elsaesser, T.; Kaiser, W. *Chem. Phys. Lett.* **1989**, *156*, 381.
(31) Whitnell, R. M.; Wilson, K. R.; Hynes, J. T. *J. Phys. Chem.* **1990**, *94*, 8625.
(32) Davis, H. F.; Lee, Y. T. *J. Phys. Chem.*, submitted for publication.
(33) Lawrence, W. G.; Clemitshaw, K. C.; Apkarian, V. A. *J. Geophys. Res.* **1990**, *95*, 18,591.